Equilibrium conversion, selectivity and yield optimization of the simultaneous liquid-phase etherification of isobutene and isoamylenes with ethanol over Amberlyst™ 35

R. Soto, C. Fité, E. Ramírez, R. Bringué and F. Cunill*

*Chemical Engineering Department. Faculty of Chemistry. University of Barcelona. Martí i Franquès 1-11, 08028-Barcelona.**Corresponding author. Tel.: +34934034769, Fax: +34934021291

Email addresses: r.soto@ub.edu (R. Soto), fite@ub.edu (C. Fité), eliana.ramirez-rangel@ub.edu (E. Ramírez), rogerbringue@ub.edu (R. Bringué), fcunill@ub.edu (F. Cunill).

Graphical abstract

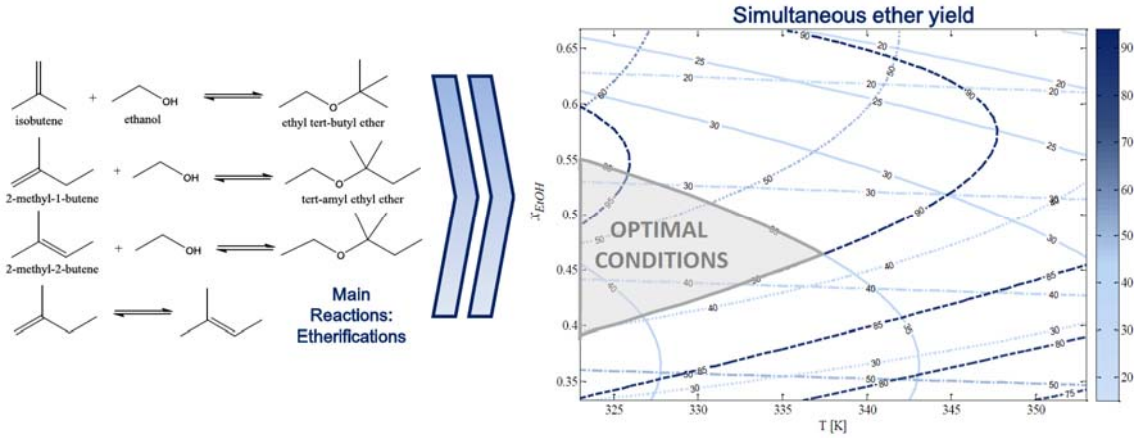

Abstract

A prospective study on the product distribution at chemical equilibrium for the simultaneous liquid-phase etherification of isobutene and isoamylenes with ethanol over Amberlyst™ 35 is presented. Experiments were performed isothermally in a 200 cm^3 stirred tank batch reactor operating at 2.0 MPa. Initial molar ratios of alcohol/olefins and isobutene/isoamylenes ranged both from 0.5 to 2, and temperature from 323 to 353 K. Reactants equilibrium conversion, selectivities and yields toward products were clearly affected by the experimental conditions. Experimental etherification yields have been modeled using the response surface methodology (RSM), combined with the stepwise regression method to include only the statistically significant variables into the model. The multiobjective optimization (MOO) of etherification yields has been carried out numerically, by means of the desirability functions approach, and graphically, by using the overlaid contour plots (OCP). Optimal conditions for the simultaneous production of ethyl *tert*-butyl ether (ETBE) and *tert*-amyl ethyl ether (TAEE) have been found to be at low temperatures (323 to 337 K) and initial molar ratio alcohol/olefins close to 0.9 and isobutene/isoamylenes close to 0.5.

Keywords: ethyl tert-butyl ether (ETBE); tert-amyl ethyl ether (TAEE); simultaneous etherification; equilibrium conversion; selectivity; yield optimization

1. Introduction

The development of new oil reserves and extraction technologies is changing the geopolitical trends and prospects of fossil fuels. Gasoline and diesel as fuels are still expected to play an important role in the present century and governments are therefore regulating fuels quality through more rigorous legislation to diminish the amount of pollutants emitted to the atmosphere from fuel combustion. The European Directive 2009/28/EC promotes the usage of combustibles from renewable resources, such as bioethanol, and the Directive 2009/30/EC itemizes the guidelines with respect to fuel reformulation. For instance, it limits the gasoline maximum content of olefins, ethanol (EtOH), *tert*-butyl alcohol (TBA) and ethers with five or more carbon atoms to 18, 10, 15 and 22 vol.%, respectively. Moreover, it limits the minimum RON (Research Octane Number) of a gasoline to 95, the maximum oxygen content to 3.7 wt.% and the maximum Reid vapor pressure (RVP) to 60 kPa (8.70 psi).

The efficiency of a gasoline fueled engine is highly influenced by the fuels antiknock characteristics, which depend essentially on the chemical composition. The adequate performance of a vehicle depends on a minimal volatility of the fuel, which can be expressed by several characteristics such as distillation curves, vapor pressure, vaporization enthalpy and the vapor/liquid ratio [1,2]. The vapor pressure of gasoline is directly related to the emission of volatile compounds from gasoline and the ensuing combustion processes, especially in starting the engine on cold days and in continuous operation in hot days.

The main pollutants emitted from gasoline are carbon monoxide (CO), carbon dioxide (CO_2), particulate matter (PM), nitrogen oxides (NO_x's) and volatile organic compounds (VOC's) [3]. NO_x's and VOC's emissions react in the presence of sunlight by means of a series of photochemical reactions involving hydroxyl-, peroxy-, and alkoxy radicals, to form ozone, a secondary and hazardous pollutant in the troposphere [4]. It is noteworthy that the main compounds responsible for the potential of tropospheric ozone formation of a gasoline (above 90%) are the C_5 isoolefins or isoamylenes (IA). These are also the olefins with the highest volatility of a gasoline, thus their reduction or substitution is environmentally advisable [5]. Several alternatives coexist to reduce the C_5 olefins content such as etherification, oligomerization and/or alkylation. Based on studies involving vehicles, it has been demonstrated that the addition of oxygenates, particularly fuel ethers such as methyl *tert*-butyl ether (MTBE), ethyl *tert*-butyl ether (ETBE), *tert*-amyl methyl ether (TAME) and *tert*-amyl ethyl ether (TAEE), reduces the emissions of CO, PM, COV's, ozone and CO_2 [6–11].

Oxygenates increase the octane index and incorporate oxygen in their composition, what contributes to a more complete combustion in the engine and thus they can be considered as substitutes for aromatics in high performance gasolines [12]. Among the main two types of oxygenates, ethers and alcohols, the former are preferred owing to their blending characteristics (Table 1) [13,14]. In general, ethylic ethers (namely ETBE and TAEE) are preferred to methylic ones due to their properties and because they are considered bioethers, since they can be manufactured from bioethanol, a renewable energy source. Gasoline oxygenated with such ethers presents a low volatility that is certainly appropriate to be used in summer time or in tropical zones. Even in the cold season, C_4 hydrocarbons can be blended with such oxy-gasoline to get an easy startup of the engine. This flexibility offers a top position in any choice of a gasoline producer, particularly compared to direct blending of alcohols [15,16].

Besides ethers and primary alcohols, tertiary alcohols such as TBA and *tert*-amyl alcohol (TAA) are also considered suitable additives due to their low volatility and their potential to reduce aldehyde formation from the combustion of gasoline-ether mixtures [17]. Despite not being oxygenates, hydrogenated dimers of isobutene (IB) and isoamylenes (IA) are also interesting chances as fuel additives because of their high octane rating and low water solubility [18,19]. For instance, 2,4,4-trimethyl-1-pentene (TMP-1) and 2,4,4-trimethyl-2-pentene (TMP-2), could be used as a feedstock to produce other high-octane gasoline components such as isooctane (2,2,4-trimethyl pentane) by means of the dimer hydrogenation or ethers like 2-methoxy-2,4,4-trimethyl pentane and 2-ethoxy-2,4,4-trimethyl pentane. In addition, dimers of IA can be used in the perfumery and flavor industry, what makes these side products valuable [20].

Table 1

Tertiary alkyl ethers are usually manufactured in equilibrium reactors. Depending on experimental conditions, a wide variety of compounds can be formed as products of reversible and irreversible reactions. To know the product distribution under different experimental conditions and at chemical equilibrium is of utmost importance for designing reaction units, such as industrial fixed-bed catalytic reactors or reactive distillation units. This is crucial not only to determine whether further separation units are required, but also to predict composition, properties and possible emissions from final blended gasoline. Several studies have been focused on the performance of isolated production of ETBE and TAEE in both absence and presence of water [25,27–30]. But there is scarce information about the simultaneous production of bioethers and, more specifically, concerning equilibrium conversion and selectivity [13,14,31–34]. Besides reducing the C_5 olefins content and using EtOH as raw material, the simultaneous production of ETBE and TAEE is a versatile and flexible process, whose

integration and intensification can provide several advantages. Furthermore, MTBE and ETBE existing plants could be easily readapted toward a new production target by revamping. Another potential resides in the possibility of using ETBE, TAEE and EtOH (in lower extent than ethers) together for direct blending with gasoline. Moreover, it has been stated that ETBE and TAEE are also useful as cosolvents to make EtOH compatible with diesel, what extends the range of application of ethylic ethers [12].

The aim of the present work is to study the feasibility of the simultaneous liquid-phase etherification of IB and IA with EtOH catalyzed by Amberlyst^{TM} 35. Modeling and optimization of etherification yield under the studied experimental conditions is a main goal, since it provides interesting information for direct application at industrial scale.

2. Experimental

2.1. Experimental Setup

Experiments were carried out in a 200 cm^3 stainless steel isothermal tank reactor equipped with a six-blade magnetic stirrer operated in batch mode. The stirring speed was set to 500 rpm. Assayed temperature ranged from 323 to 353 K, controlled within ± 0.1 K by a thermostatic bath mixture (33 vol.% of 1,2-propanediol, 67% of water) fed to the reactor jacket. The pressure was set to 2.0 MPa by means of N_2 to maintain the reacting mixture in the liquid phase. One reactor outlet was directly connected to a gas chromatograph (GC) for sampling. More detailed information about the experimental setup can be found elsewhere [31].

2.2. Chemicals

A mixture of IA containing 2M2B (96% G.C.) and 2M1B (4% G.C.) (TCI Europe, Belgium), isobutene (>99.9% G.C., Air Liquide, Spain), absolute EtOH (max. 0.02 wt.% of water, Panreac, Spain) and deionized water were used as the initial reaction mixture in all experimental runs.

The following chemical standards were used for the calibration of the system: TMP-1 (>98.0% G.C., Fluka, Buchs, Switzerland) and TMP-2 (>98% G.C., Fluka, Buchs, Switzerland), TAA (>98.0% G.C., TCI Europe, Belgium), TBA (>99.7% G.C., TCI Europe, Belgium), ETBE (>99.0% G.C., TCI Europe, Belgium), 2M1B (>99.0% G.C., TCI Europe, Belgium) and 2M2B (>99% G.C., Sigma Aldrich, Germany). TAEE was obtained in our laboratory by distillation with a minimum purity of 98.5% G.C. Dimers C_5 were also synthetized and purified in our laboratory (>99% G.C.). Due to the difficulty of purifying $C_{4\text{-}5}$ codimers, their chromatographic response was estimated as an intermediate response factor between C_4 and C_5 dimers.

2.3. Catalyst

Amberlyst^{TM} 35 (A-35, Rohm & Haas, Chauny, France) was used as the catalyst. It is a macroreticular acidic ion-exchange resin, widely used in etherification processes, for which excellent results in the isolated synthesis of ETBE and TAEE have been reported [28,35]. In the pretreatment, the catalyst was dried for 2.5 h in an atmospheric oven at 383 K and subsequently 15 h in a vacuum oven at 373 K. The residual amount of water in the catalyst was measured by Karl Fisher titration method (Orion AF8 volumetric Karl Fisher titrator, Thermo Electron Corporation, Massachusetts, US) for different samples of A-35 with a result of less than 3.5 wt.% of water. In systems catalyzed by ion-exchange resins, internal mass transfer resistances may appear when using commercial bead size distributions. As a result, reaction rate decreases in the progress toward equilibrium. This hindrance usually increases with temperature and particle size. For instance, for the isolated synthesis of ETBE from pure IB feed at 363 K, the effectiveness factors for A-35 particles ranging 0.63-0.8 mm and 0.4-0.63 mm have been reported to be 0.54 and 0.73, respectively [28]. In the present work, catalyst was used as commercially shipped, with the following cumulative bead size distribution, relative to the measured number of particles: 422 μm (<10%), 466 μm (<25%), 531 μm (<50%), 619 μm (<75%), and 716 μm (<90%) [14]. In this work, possible internal mass transfer limitations were not considered as a drawback, since it is focused on products selectivities and yields at chemical equilibrium, and the commercial size distribution is of industrial interest. The relevant physical and structural properties of A-35 are acid capacity (5.32 eq H^+/kg), BET surface area (34.0 $m^2 \cdot g^{-1}$), mean BET pore volume (0.21 $cm^3 \cdot g^{-1}$), and maximum operating temperature (423 K).

2.4. Analytical Method

Samples were taken inline from the reaction medium through a liquid sampling valve (Valco A2CI4WE.2, VIVI AG International, Schenkon, Switzerland), which injected 0.2 μL into a gas-liquid chromatograph (Agilent 6890GC, Madrid, Spain) equipped with a capillary column (HP-PONA 19091S-001, Hewlett Packard, Palo Alto, USA.; 100% dimethylpolysiloxane, 50.0 m x 0.2 mm x 0.5 μm nominal). A mass selective detector (HP 5973N MS) coupled to the GC was used to identify and quantify the reaction system components. The oven temperature was programmed with a 10 min hold at 304 K, followed by a 20 $K \cdot min^{-1}$ ramp, from 304 to 353 K, a subsequent second hold of 5 min followed by a second temperature ramp of 60 $K \cdot min^{-1}$ from 353 to 493 K. The final temperature was held for 10 min. Helium (99.998% Abelló-Linde, Barcelona, Spain) was used as carrier gas. Since several $C_{4\text{-}5}$ and C_5 dimers were formed, $C_{4\text{-}5}$ codimers on one side and C_5 dimers on another were respectively lumped together. Neither trimers nor higher oligomers were detected under the conditions of this study.

2.5 Procedure

The initial molar ratio of alcohol/olefins ($R_{A/O}$) and isobutene/isoamylenes ($R_{C4/C5}$) were both varied between 0.5 and 2. A fixed water amount of 1 wt.% of the total reactant mixture was initially added to every experiment to monitor TBA and TAA formation and to approach industrial conditions in which the alcohol stream would contain small amounts of water. Assayed reaction temperatures were in the range of 323 to 353 K. These particular conditions were chosen because they are similar to those of industrial interest in etherification processes. The catalyst load varied between 4 and 8 g in order to reach chemical equilibrium during the experimental runs. The possible effect of the catalyst load was studied in a previous work [31], where it was concluded that it can be neglected for the used range of loads.

Firstly, EtOH, water and the catalyst were placed into the reactor and the stirrer was turned on. Then, the reactor was heated up by the thermostatic bath until the system reached the desired temperature. Known amounts of IA and IB were introduced in a calibrated burette and pressurized to 1.5 MPa with nitrogen. Once the temperature was reached inside the reactor, the mixture of olefins was shifted from the burette into the reactor. Then the reactor pressure was set to 2.0 MPa with nitrogen to ensure the liquid phase, and the reactor was heated up until it reached the desired temperature again. During the experimental runs the reactor operated isothermally. For the measurement of the reaction mixture composition, samples were taken and analyzed periodically until pseudo-equilibrium state was reached (typically after 6-8 h of running). A total of 44 experimental runs were carried out.

2.6 Theory and Calculations

Reactants conversion, selectivity and yield toward products were calculated at each instant for each run by means of the following expressions:

$$X_j = \frac{mole\ of\ j\ reacted}{initial\ mole\ of\ j} \quad (1)$$

$$S_j^k = \frac{mole\ of\ k\ produced}{mole\ of\ j\ reacted} \quad (2)$$

$$Y_j^k = X_j \cdot S_j^k \quad (3)$$

where *j* refers to the reactant and *k* to the considered product or byproduct.

In order to estimate the experimental error, the experiments at $R_{A/O} = R_{C4/C5} = 1$ were replicated. In general, the 95% confidence interval for the means of conversion, selectivity and yield was found to be less than 6%. Due to the low selectivity values toward tertiary alcohols, a larger uncertainty was observed for S_{IB}^{TBA} and S_{IA}^{TAA} (14 and 16%, respectively). Mass balance

was fulfilled in all the runs within ±6%. Globally, experiments have been considered reproducible and the results as reliable.

The response surface methodology (RSM) is a useful technique in the solution of many problems of the chemical industry. For instance, one important application is the modeling and optimization of industrial processes [36,37]. It is a valuable tool to determine the experimental conditions for which the throughput toward a desirable chemical product is the maximum attainable. A second order polynomial expression with interaction terms was used for the modeling of the experimental etherification yields:

$$y_n(z) = \beta_0 + \sum_{m=1}^{n} \beta_m z_m + \sum_{m=1}^{n} \beta_{mm} z_m^2 + \sum \sum_{l<m=2}^{n} \beta_{lm} z_l z_m \qquad n=1,2.3...r \qquad (4)$$

where z_1, z_2, …, z_k are the coded variables that refer to the experimental conditions, and β_0, β_m, β_{mm} and β_{lm} are fitting parameters. A confidence level of 95% was used to assess the statistical significance of fitted polynomial models. The number of variables of Eq.4 was reduced to the minimum statistically significant by means of the stepwise regression procedure [38] using the software Design-Expert v9. The significance level for each parameter to be either included or rejected from the final equation was set to 0.05. This technique has been demonstrated to be effective when selecting a predictive equation that comprises the fewest possible variables to determine reliable process values.

Since four different responses are obtained in the modeling of etherification yields, the simultaneous optimization of all of them results in a multi-objective optimization (MOO) problem. The conditions for which the yield to ETBE is maximum may differ from those for which the yield to TAEE is maximum. The overall objective is to find out the conditions that globally maximize the yield toward both ethers. A relatively straightforward approach in MOO is to overlay the contour plots (OCP) for each target response [37], where a region near "optimal" is obtained rather than a unique optimum point [39]. On the other hand, the desirability function approach is a useful numerical technique for the analysis of experiments in which several responses have to be optimized simultaneously. Originally developed by Harrington (1965) [40] and modified by Derringer and Suich (1980) [41], the main concept of the desirability function is to transform a multiresponse problem into a single response problem. Once all the responses $Y_n(z)$ have been fitted to polynomials by RSM, an individual desirability function $d_n(Y_n(z))$, ranging between 0 and 1, is assigned for each response $Y_n(z)$. For the two sided case and considering the maximization of $Y_n(z)$, the individual desirability function is expressed as follows:

$$d_n(Y_n(z)) = \begin{cases} 0 & if\ y_n(z) < L_n \\ \left(\dfrac{y_n(z) - L_n}{T_n - L_n} \right)^s & if\ L_n \geq y_n(z) \geq T_n \\ 1 & if\ y_n(z) > T_n \end{cases} \qquad (5)$$

where z are the factors, L_n is the lower acceptable value of $Y_n(z)$, and T_n is the target value. The parameter s is user specific weight factor that determines the shape of the desirability function: it takes values either higher or lower than unity, depending on the higher or lower relative importance assigned to the response. The parameter s can be set equal to unity for all responses when equal importance is assigned to each. An overall objective function, the total desirability $D(z)$, can be defined as the geometric mean of the individual desirabilities obtained for the r responses of interest, as follows:

$$D(z) = \sqrt[r]{\prod_{n=1}^{r} d_n(Y_n(z))} \qquad (6)$$

3. Results and Discussion

3.1 Description of the reaction system

The simultaneous etherification of IB and IA with EtOH is a complex reaction system in which several chemical reactions can take place simultaneously depending on the experimental conditions (Figure 1). The main reactions are the etherification of EtOH with IB (R1) and IA (R2 and R3), and the double bond isomerization reaction (R4) between both IA (2M1B and 2M2B). Equilibrium constants of reactions R1 to R4, and related thermodynamical properties, have been already estimated and discussed in a previous work [31]. Since water is present in the initial reactant mixture (1 wt.%), hydration of IB and IA (R5, R6 and R7) could also take place to form tertiary alcohols, namely TBA and TAA. Diethyl ether (DEE) could be formed by dehydration of two EtOH molecules (R8). Since DEE formation was detected only at 353K and $R_{A/O}$=2 and in very small amount (less than 0.06% G.C.), DEE was not included neither in the system calibration nor in further calculations. IB (C_4) and IA (C_5) dimers and codimers thereof ($C_{4\text{-}5}$) can be formed by reactions R9, R11 and R12. This products were detected only under initial olefin stoichiometric excess ($R_{A/O}$=0.5) at the higher explored temperatures. As C_4 dimers, only TMP-1 and TMP-2 were detected, whereas a wide variety of compounds were identified as $C_{4\text{-}5}$ codimers and C_5 dimers. Double bond isomerization reaction between TMP-1 and TMP-2 is also expected to take place (R10).

Figure 1

In the experimental runs, ETBE and TAEE were always formed. ETBE was the main reaction product in terms of mole, followed by TAEE. The main side products were tertiary alcohols (TBA and TAA) and dimerization products. Dimerization proceeded so slowly that the molar fractions of the involved compounds in a relatively short time period can be considered to be almost constant, what constitutes a pseudo stationary state.

3.2 Effect of temperature

Since the main etherification reactions involved in this study are exothermic (R1-R3) [31], reactants equilibrium conversion, X_j, is expected to decrease on increasing temperature. Although reaction equilibrium constants depend only on temperature, reactants conversion at equilibrium situation is given by initial composition and operating temperature. As depicted in Figure 2, the higher the temperature, the lower the reactants equilibrium conversion. Compared to X_{IB}, a significantly lower X_{IA} (about a half) was reached, what indicates that ETBE synthesis from IB and EtOH is thermodynamically favored compared to that of TAEE from IA and EtOH. Under stoichiometric conditions between alcohols and olefins ($R_{A/O}$=1), X_{EtOH} values at equilibrium were between X_{IB} and X_{IA}. This is consistent with the equilibrium constants values of these etherification reactions estimated in a previous work [31]: equilibrium constants of ETBE formation (R1) are higher than those of TAEE formation (R2 and R3) at every temperature. A steeper decrease of X_{IA} on increasing temperature was observed at $R_{A/O}$=2 (Figure 2c and d) and it suggests that TAEE formation is more affected by temperature changes than that of ETBE. Globally, X_{IB}, X_{IA} and X_{EtOH} values ranged between 69.8% and 97.9%, between 17% and 65.6% and between 32.3% and 97.0%, respectively. The effect of temperature on X_{IA} was in good agreement with that reported for the isolated etherification of IA with EtOH under similar conditions [42].

Figure 2

The effect of temperature on reactants selectivity toward products is shown in Figure 3. Remarkably high values of S_{IB}^{ETBE} and S_{IA}^{TAEE} (always >90%) were obtained, which did not depend significantly on temperature. This is undoubtedly a desirable industrial performance to obtain both ethers. Both S_{IB}^{ETBE} and S_{IA}^{TAEE} decreased smoothly at increasing temperature, whereas S_{IB}^{TBA} and S_{IA}^{TAA} followed an opposite trend. S_{IB}^{ETBE} values were always slightly higher than those of S_{IA}^{TAEE}, what is related to the fact that S_{IA}^{TAA} values were slightly higher than S_{IB}^{TBA} values. Regarding products from EtOH, the reaction system was generally more selective toward ETBE than toward TAEE. This difference is consistent with a larger equilibrium constant of ETBE formation compared to TAEE formation [31], and it is even more noticeable at higher temperature.

Figure 3

3.3 Effect of $R_{A/O}$

The effect of $R_{A/O}$ on reactants equilibrium conversion is illustrated in Figure 4. The highest X_{EtOH} was obtained at $R_{A/O}$=0.5 and the highest olefins equilibrium conversion were reached at stoichiometric excess of EtOH ($R_{A/O}$=2), but at the expense of lower X_{EtOH}. X_{IA} was more sensitive to temperature changes than X_{IB}.

Figure 4

The effect of $R_{A/O}$ on reactants selectivity toward products at equilibrium is shown in Figure 5. S_{IB}^{ETBE} and S_{IA}^{TAEE} were high and increased slightly on increasing $R_{A/O}$. On the contrary, S_{IB}^{TBA} and S_{IA}^{TAA} were low and followed an opposite trend with $R_{A/O}$. The highest value of S_{EtOH}^{ETBE} was obtained at $R_{A/O}$=0.5 and the highest value of S_{EtOH}^{TAEE} was reached at $R_{A/O}$=2. As seen in Figure 5a and b, the shape of selectivity profile vs. $R_{A/O}$ was very similar at 343 and 353K, the main difference being the extent in which dimerization products were formed. The selectivity profiles obtained at 323 and 333K were similar to those plotted in Figure 5, but without noticeable formation of dimers. The effect of $R_{A/O}$ on byproducts formation will be further discussed in the side products section.

Figure 5

3.4 Effect of $R_{C4/C5}$

Figure 6 depicts the dependence of reactants conversion on $R_{C4/C5}$. As the initial IB concentration increased, lower values of X_{IB} and X_{IA} were obtained whereas X_{EtOH} was slightly higher. The effect of $R_{C4/C5}$ on reactants equilibrium conversion was more noticeable at $R_{A/O}$=1 (see Figure 6c). The overall effect of $R_{C4/C5}$ on reactants equilibrium conversion was less pronounced than those of temperature and $R_{A/O}$.

Figure 6

The effect of $R_{C4/C5}$ on reactants selectivity is shown in Figure 7. S_{IB}^{ETBE} and S_{IA}^{TAEE} values at equilibrium were high, and decreased smoothly on increasing $R_{C4/C5}$. Concerning EtOH, S_{EtOH}^{ETBE} increased with $R_{C4/C5}$ and accordingly S_{EtOH}^{TAEE} followed the opposite trend. Thus, it can be concluded that increasing $R_{C4/C5}$ chiefly favors ETBE formation. Similar values of S_{EtOH}^{ETBE} and S_{EtOH}^{TAEE} were obtained at $R_{C4/C5}$=0.5 and $R_{A/O}$=2, see Figure 7a. The effect of $R_{C4/C5}$ on olefins

selectivity toward dimerization products was enhanced at high temperatures and $R_{A/O}$=0.5 (Figure 7b).

Figure 7

3.5 Side reactions

3.5.1 Tertiary alcohols formation

The initial water present in the reaction medium (1 wt.%) reduced obviously the olefins selectivity to ethers. S_{IA}^{TAA} and S_{IB}^{TBA} values at equilibrium were always lower than 13 and 9%, respectively. As can be observed in Figure 8, S_{IA}^{TAA} was always higher than S_{IB}^{TBA}. Nevertheless, at $R_{C4/C5}$=1 and at equilibrium, a larger amount of mole of TBA was formed compared to TAA, what indicates that TBA formation is thermodynamically favored in front of TAA formation. These results are in concordance with the larger equilibrium constants values for TBA synthesis (R5) [43] compared to TAA synthesis from 2M1B and 2M2B (R6 and R7) [27, 43].

The effect of the reaction temperature on tertiary alcohols formation is presented in Figure 8a. Both S_{IB}^{TBA} and S_{IA}^{TAA} increased smoothly with temperature. This fact is in good agreement with published results, where an increase of S_{IB}^{TBA} with temperature was observed in the synthesis of ETBE [25] and in the synthesis of isopropyl *tert*-butyl ether [44]. The selectivity obtained at equilibrium is a result of the temperature, the initial composition and all reactions taking place. Despite the known exothermicity of olefins hydration, etherification of olefins are known to present a value of the thermodynamic equilibrium constant higher than the corresponding olefin hydration [27,43, 45], that can explain the enhancing effect of temperature on S_{IB}^{TBA} and S_{IA}^{TAA}.

Figure 8

Figure 8b plots the effect of $R_{A/O}$ on the formation of tertiary alcohols. Both S_{IB}^{TBA} and S_{IA}^{TAA} decreased on increasing $R_{A/O}$. This is because as $R_{A/O}$ increases, lower amount of olefins is initially present in the reaction media and therefore lower amount of tertiary alcohols is formed by olefins hydration. The effect of $R_{C4/C5}$ on tertiary alcohols formation is depicted in Figure 8c. S_{IB}^{TBA} increased slightly on increasing $R_{C4/C5}$ whereas S_{IA}^{TAA} followed an opposite trend. The explanation of this fact arises from the initial IB concentration, as it increased, water was preferably consumed to form TBA rather than TAA.

3.5.2 Dimers and codimers formation

Irreversible formation of dimerization products was detected only at initial olefin stoichiometric excess ($R_{A/O}$=0.5) and high temperature (343 and 353 K), as a result of the higher sensitivity of this side reactions to temperature (Figure 5). This is consistent with previous studies focused on the IB and IA dimerization that concluded that polar conditions (induced, namely, by water and alcohol presence in the present study) inhibit oligomerization reactions [14,44,46]. Both TMP-1 and TMP-2 were formed through isobutene dimerization (R9). In addition, isomerization between both diisobutenes (R10) also took place, the formation of TMP-1 being favored, since TMP-1 is a more stable molecule than TMP-2 due to the internal repulsions caused by the large size of the *tert*-butyl group in the TMP-2 molecule [47,48]. As observed in Figure 9a, when C4 dimers were forms, the TMP-1/TMP-2 molar ratio was around 4 at the end of runs, consistent with published results [47] and with the thermodynamic equilibrium constant for trimethylpentenes isomerization (R10), which are in the range from 0.26 to 0.29 for the assayed temperatures [31]. From IA dimerization (R12 in Figure 1), a wide variety of diisoamylenes can be formed [49]. Additionally, codimerization between IB and IA (R11 in Figure 1) also occurred. As observed in a previous work [14], dimers formation took place almost linearly with time and the formed mole of C8 dimers and C9 codimers was very similar at $R_{C4/C5}$=1, which suggests competitive adsorption between IB and IA. The largest amount of dimers was detected at $R_{A/O}$= 0.5, $R_{C4/C5}$=2 and 353 K.

Figure 9

The effect of $R_{C4/C5}$ on dimers formation is illustrated in Figure 9b. The total values of IB and IA selectivities toward dimerization products (dimers and codimers) were always lower than 8% and 10%, respectively. However, IB always yielded larger amounts of dimers than IA in terms of mole, as seen in Figure 9a. As $R_{C4/C5}$ increased, the amount of C_4 and $C_{4\text{-}5}$ dimers detected at the end of the runs did it as well. It is explained by the larger amount of IB available in the bulk phase. So it can be stated that IB concentration is a determinant factor for dimerization in the present system. The effect of initial IA concentration on dimers formation was less noticeable.

3.6 Modeling and optimization of etherification yields

The reaction yield is a suitable parameter to measure the industrial feasibility, which considers simultaneously reactants conversion and selectivity (Eq. 3). Experimental etherification yield data were modeled using RSM to fit such responses with respect to reaction temperature and initial composition. A second order polynomial form (Eq. 4) was fitted to experimental yield data by means of the stepwise regression procedure. In order to center the

variables of the experimental design, both initial molar ratios of $R_{A/O}$ and $R_{C4/C5}$ were translated into initial molar fractions of alcohol in the initial reactant mixture (x_A) and of IB in the initial olefins mixture (x_{C4}). The experimental yield data modeled are gathered in Appendix 1 from Supplementary Material section. Tables 2 and 3 show the analysis results in terms of coded variables for the regression coefficients and the models obtained. As it can be seen, the analysis of variance (ANOVA) revealed that the proposed empirical models were adequate to express the actual relation between the responses and significant variables, with high values of adjusted R^2. The significance level for each equation variable was evaluated by its *p*-value and the significance level of each empirical model by the test of Fisher (*F*-value). Residual plots confirmed the randomness of the residuals for each model (see Supplementary Material, Appendix 2). Experimental data vs. predicted value plots also confirmed the suitability of the fitted equations (see Figure 10). The largest deviations were found for the modeling of Y_{IB}^{ETBE} at the highest temperatures, what is attributed to the higher amount of formed dimers.

Table 2

Table 3

The empirical equations obtained for etherification yields in terms of non-coded variables (Eqs. 7-10), refer to the expressions with the minimum number of terms in which all parameters and the regression itself are statistically significant at a confidence level of 95%. *T* is expressed in K in these equations. With respect to the effects for each model, the linear terms *T*, x_A and x_{C4}, the quadratic effect x_A^2 and the interaction effect of $x_A \cdot x_{C4}$ showed the highest level of statistical significance for the fitted equations. The quadratic effect x_{C4}^2 was only significant for Y_{EtOH}^{TAEE}. Finally, the interaction effect $T \cdot x_A$ was only significant for the olefins yield toward ethers. Globally, increasing the temperature, decreased both Y_{IB}^{ETBE} and Y_{IA}^{TAEE}. Y_{EtOH}^{ETBE} resulted almost independent of temperature.

$$Y_{IA}^{TAEE} = -50.12 + 0.094 \cdot T + 663.21 \cdot x_A - 115.37 \cdot x_{C4} - 225.36 \cdot x_A^2 + 52.92 \cdot x_{C4}^2 - 1.15 \cdot T \cdot x_A + 95.11 \cdot x_A \cdot x_{C4} \quad (7)$$

$$Y_{IB}^{ETBE} = 235.77 - 0.559 \cdot T + 27.53 \cdot x_A - 95.68 \cdot x_{C4} - 245.07 \cdot x_A^2 + 0.588 \cdot T \cdot x_A + 147.62 \cdot x_A \cdot x_{C4} \quad (8)$$

$$Y_{EtOH}^{TAEE} = 235.91 - 0.512 \cdot T + 86.35 \cdot x_A - 354.02 \cdot x_{C4} - 190.52 \cdot x_A^2 + 33.93 \cdot x_{C4}^2 + 0.556 \cdot T \cdot x_{C4} + 158.27 \cdot x_A \cdot x_{C4} \quad (9)$$

$$Y_{EtOH}^{ETBE} = 59.15 - 0.07 \cdot T - 54.665 \cdot x_A + 155.2 \cdot x_{C4} - 160.88 \cdot x_A \cdot x_{C4} \quad (10)$$

Figure 10

The ability of the empirical models to predict product yields has been confirmed by carrying out an additional run under slightly different conditions, but within the assayed experimental range. More specifically, the run was caried out at $R_{A/O}$=1.5, $R_{C4/C5}$=1.5 and 343 K. Experimental etherification yields obtained were compared to those predicted by the empirical models (Eqs. 7-10), the largest deviation being around 5% for Y_{IA}^{TAEE}.

Using the obtained models, response surfaces and their contour plots were constructed for the pair of factors T and x_A (the most influencing factors) while holding the third factor, x_{C4}, constant. An example of the response surface profiles obtained and the corresponding contour plots are shown in Figure 11. As can be seen the proposed models fit experimental data in a reasonably good way.

Figure 11

The optimization of the experimental conditions that simultaneously maximize etherification yields was carried out graphically by the overlaid contour plots (OCP) holding constant x_{C4} at 0.333, 0.5 and 0.666. Figure 12 represents an example of the OCP obtained. The grey shadowed area highlights the optimal experimental region that simultaneously maximizes all etherification yields. It was observed that this area is shifted to higher values of x_A when x_{C4} increases, which should be due to IB dimers formation. In other words, a larger initial amount of polar component (EtOH) is required to avoid expected formation of diisobutenes on increasing the initial IB concentration. This methodology reported the best results for x_{C4}=0.333, x_A ranging from 0.4 to 0.55 and temperature ranging from 323 to 337 K. However, a large grade of inaccuracy arises from these plots since the optimal region limited between the contour levels is subjected to a deal of subjectivity. Furthermore, separated analysis is required for each value of x_{C4}.

Figure 12

For the sake of contrasting results and obtaining more accurate data, numerical MOO was also made by solving the overall desirability $D(x)$ function obtained from the individual desirability functions. After using RSM to fit appropriate polynomial models to the r responses $Y_n(z)$, Eqs. 7-10, individual desirability functions $d_n(Y_n(z))$ were defined for each response using Eq. 5. The value of s was set to the unity to assign equal weight to each response and the same priority has been therefore given to the production of ETBE and TAEE. Other criteria could be applied, such as giving priority to olefins yield toward ethers or depending on reactants price and availability. However, the present MOO has been focused from an academic standpoint and so raw materials price has not been considered. Eigenvalues analysis described in Khuri and

Cornell [39] was made prior to numerical optimization in order to evaluate the linear correlation between responses showing that responses were not linearly correlated. The constraints applied to the experimental variables for the optimization of overall $D(x)$ were set to obtain results within the range of assayed experimental conditions: $0.333<x_A<0.666$, $0.333<x_{C4}<0.666$ and $323<T<353$. Obtained numerical results for each $d_n(Y_n(z))$ and $D(x)$ are summarized in Table 4. Figure 13 plots the contour plot obtained for the overall desirability $D(x)$ at $x_{C4}=0.333$. As can be seen the shape of $D(x)$ delimits as well an optimal region of x_A and T in which the maximum values of etherification yields are attained.

Table 4

Figure 13

From numerical optimization values of $R_{A/O}=0.86$, $R_{C4/C5}=0.5$ and T=323 K were estimated as the experimental conditions that maximize the simultaneous production of ETBE and TAEE. Perhaps, the obtained value of $R_{A/O}=0.86$ is somewhat low compared to the $R_{A/O}$ value used in isolated production of tertiary alkyl ethers, typically 1.05 [50], because a slight excess of EtOH would prevent dimerization reactions and would enhance olefins conversion. Moreover, $R_{A/O}=1$ represents the stoichiometric ratio of etherification reactions. Nevertheless, it is to be highlighted that an initial 1 wt.% of water was used in all the experiments of the present work, thus an additional amount of olefins were consumed in hydration reactions and that could explain the slight excess of olefins obtained by numerical MOO. Besides, the obtained values of T=323 K and $R_{C4/C5}=0.5$ imply a reduction of olefins dimerization production, because, as seen before, IA concentration is not as critical factor for dimerization as IB concentration. Based on these reasons, obtained results from numerical MOO are considered plausible and unbiased.

According to the optimal region determined by the OCP methodology at $x_{C4}=0.333$, optimal range of temperature to produce simultaneously ETBE and TAEE ranges from 323 to 337 K and $R_{A/O}$ from 0.64 to 1.22. These values are coherent with those determined numerically by the desirability function approach. Finally, the sensitiveness of $D(x)$ on varying experimental conditions (Table 4), revealed that x_{C4} can be varied from 0.333 to 0.666 and the obtained values for $D(x)$ are still higher than 0.67. Thus $R_{C4/C5}$ could be set depending on both, the refinery necessities (preferred production of ETBE or TAEE) and the provisioning of C_4 and C_5 olefinic streams.

The applied methodology can be particularly useful when modeling yields in units that produce several desired products simultaneously. In that case, numerical MOO using desirability functions can help to decide how much in the yield of a certain product is the

engineer willing to reduce for a gain in the yield of other products. Also to find out the experimental conditions that give priority to special production targets.

4. Conclusions

Experimental equilibrium data presented in this paper would represent the output composition of industrial equilibrium reactors and thus represent valuable information. Reactants equilibrium conversion decreases on increasing the temperature, as expected for exothermic reactions. Increasing $R_{A/O}$, higher olefins equilibrium conversion can be achieved but at the expense of lower X_{EtOH}. Increasing $R_{C4/C5}$ slightly increases X_{EtOH} and favors ETBE formation over TAEE one. As a whole, X_{IB}, X_{IA} and X_{EtOH} ranged from 69.8 to 97.9%, from 17 to 65.6% and from 32.3 to 97.0%, respectively, depending on initial composition and temperature. The simultaneous etherification performed is a feasible technique to convert up to 65% of the environmentally troublesome C_5 isoolefins and entails large EtOH use as raw material.

High values of olefins selectivity toward target products are obtained which is certainty desirable from an industrial standpoint. A temperature increase promotes formation of both tertiary alcohols and dimerization products, whereas a $R_{A/O}$ increases shows an opposite effect on the formation of both side products. $R_{A/O}$ is, therefore, an important control variable to avoid side reactions. The effect of $R_{C4/C5}$ on side products formation is less noticeable, but an increase in IB concentration is a critical factor toward dimers formation at high temperatures.

The experimental yield data have been empirically modeled using the response surface methodology, which allows to obtain expressions able to predict etherification yields within the experimental conditions. Two different approaches have been applied to the multiobjective optimization of the overall ether yield. The obtained results from both methodologies are in reasonable agreement. Consequently, it has been concluded that the experimental conditions that maximize the simultaneous production of both ETBE and TAEE are at initial molar ratios $R_{A/O}$=0.9, $R_{C4/C5}$=0.5, and at temperature 323 K.

Acknowledgement

The authors are grateful to Rohm & Haas France SAS (The Dow Chemical Company) for providing the ion-exchange resin Amberlyst™ 35 used in this work.

Notation

2M1B	2-methyl-1-butene
2M2B	2-methyl-2-butene
A-35	macroporous ion exchange resin Amberlyst™ 35

$D(z)$	overall desirability function
$d_n(Y_n(z))$	individual desirability function for each response
DEE	diethyl-ether
ETBE	ethyl *tert*-butyl ether
EtOH	ethanol
GC	gas chromatograph
IA	isoamylenes
IB	isobutene
MOO	multi-objective optimization
OCP	overlaid contour plots
$R_{A/O}$	initial molar ratio of alcohols to olefins (dimensionless)
$R_{C4/C5}$	initial molar ratio of isobutene to isoamylenes (dimensionless)
RSM	response surface methodology
RVP	Reid vapor pressure
t	reaction time [min]
T	temperature [K]
T_b	boiling point [K]
TAEE	*tert*-amyl ethyl ether
TAA	*tert*-amyl alcohol
TBA	*tert*-butyl alcohol
TMP-1	2,4,4-trimethyl-1-pentene
TMP-2	2,4,4-trimethyl-2-pentene
X_j	conversion of reactant *j* at chemical equilibrium
S_j^k	selectivity of reactant *j* toward product *k* at chemical equilibrium
s	user specific weight factor
$Y_n(z)$	response *n* to be optimized
Y_j^k	yield of reactant *j* toward product *k* at chemical equilibrium
x_A	molar fraction of alcohol in the initial reactant mixture
x_{C4}	molar fraction of isobutene in the initial olefin mixture
z	set of variables of the experimental conditions

Greek letters

β	*regression coefficients*

References

[1] M. Le Breton, Hot and cold fuel volatility indexes of french cars: A cooperative study by the GFC volatility group, SAE Tech. Pap. 841386, 1984. DOI:10.4271/841386.

[2] L. Gibbs, Motor gasolines technical teview (FTR-1), Chevron Corporation, 2009.

[3] R. da Silva, R. Cataluña, E.W. de Menezes, D. Samios, C. Piatnicki, Effect of additives on the antiknock properties and Reid vapor pressure of gasoline, Fuel. 84 (2005) 951–9.

[4] J.S. Gaffney, N.A. Marley, The impacts of combustion emissions on air quality and climate - From coal to biofuels and beyond, Atmos. Environ. 43 (2009) 23–36.

[5] K.L. Rock, T. de Cardenas, L. Fornoff, C5 olefins. The new refinery challenge, Fuel Reformul. 2 (1992) 42–8.

[6] R.M. Reuter, J.D. Benson, V.R. Burns, R.A.J. Gorse, A.M. Hochhauser, W.J. Koehl, Effects of oxygenated fuels and RVP on automotive emissions, Auto/Oil Air Quality Improvement Program, SAE Tech. Pap. (1992) 391–412.

[7] R.F. Sawyer, Reformulated gasoline for automotive emissions reduction, Symp. Combust. 24 (1992) 1423–32.

[8] T.W. Kirchstetter, B.C. Singer, R.A. Harley, G.R. Kendall, W. Chan, Impact of Oxygenated Gasoline Use on California Light-Duty Vehicle Emissions, Environ. Sci. Technol. 30 (1996) 661–670.

[9] EFOA - Home - EFOA. http://www.efoa.eu/ (accessed June 30, 2015).

[10] T. Higgins, P. Steiner, Study on Relative CO_2 savings comparing Ethanol and TAEE as a gasoline component, Hart Energy Consulting, 2010.

[11] R. Magnusson, C. Nilsson, The influence of oxygenated fuels on emissions of aldehydes and ketones from a two-stroke spark ignition engine, Fuel. 90 (2011) 1145–1154.

[12] E.W. de Menezes, R. da Silva, R. Cataluña, R.J.C. Ortega. Effect of ethers and ether/ethanol additives on the physicochemical properties of diesel fuel and on engine tests, Fuel, 85 (2006) 815–822.

[13] R. Soto, C. Fité, E. Ramírez, R. Bringué, M. Iborra, Green metrics analysis applied to the simultaneous liquid-phase etherification of isobutene and isoamylenes with ethanol over Amberlyst™ 35, Green Process. Synth. 3 (2014) 321-333.

[14] R. Soto, C. Fité, E. Ramírez, J. Tejero, F. Cunill, Effect of water addition on the simultaneous liquid-phase etherification of isobutene and isoamylenes with ethanol over Amberlyst™ 35, Catal. Today 256 (2015) 336-346.

[15] M.N. Petre, The potential environmental benefits of utilising oxy-compounds as additives in gasoline, a laboratory based study, Environ. Health-Emerging Issues Pract. (2012) 147–176.

[16] M.N. Petre, P. Rosca, R. Dragomir. The Effect of Bio-ethers on the Volatility Properties of Oxygenated Gasoline, Rev. Chim. 62 (2011) 567–574.

[17] F. Cunill, M. Vila, J.F. Izquierdo, M. Iborra, J. Tejero, Effect of water presence on methyl tert-butyl ether and ethyl tert-butyl ether liquid-phase syntheses, Ind. Eng. Chem. Res. 32 (1993) 564–569.

[18] M.L. Honkela, A.O.I. Krause, Influence of polar components in the dimerization of isobutene, Catal. Lett. 87 (2003) 113–9.

[19] V.J. Cruz, F. Cunill, J.F. Izquierdo, J. Tejero, M. Iborra, R. Bringué, C. Fité, Los diisoamilenos como aditivos de las gasolinas, Ing. Quim. 436 (2006) 100-107.

[20] M.M. Sharma, Some novel aspects of cationic ion-exchange resins as catalysts, React. Funct. Polym. 26 (1995) 3–23.

[21] W.J. Piel, Expanding refinery technology leads to new ether potential. Fuel Reformul Nov/Dec (1992) 34–40.

[22] T. Doğu, D. Varişly, Alcohols as alternatives to petroleum for environmentally clean fuels and petrochemicals, Turkish J. Chem. 31 (2007) 551–567.

[23] H.L. Brockwell, P.R. Sarathy, R. Trotta, Synthesize ethers, Hydrocarb. Process. 70 (1991) 133–141.

[24] A. S. Hamadi, Selective additives for improvement of gasoline octane number, Tikrit J. Eng. Sci. 17 (2010) 22-35.

[25] J.H. Badia, C. Fité, R. Bringué, E. Ramírez, F. Cunill, Byproducts formation in the ethyl tert-butyl ether (ETBE) synthesis reaction on macroreticular acid ion-exchange resins, Appl. Catal. A: Gen. 468 (2013) 384–394.

[26] J.R. Peterson, Alkylate is key for cleaner burning gasoline, Natl. Meet. Am. Chem. Soc., Leawood, 41(1996) 916–921.

[27] J.A. Linnekoski, A.O.I. Krause, L.K. Struckmann, Etherification and hydration of isoamylenes with ion exchange resin, Appl. Catal. A: Gen. 170 (1998) 117–126.

[28] R. González, Performance of Amberlyst™ 35 in the synthesis of ETBE from ethanol and C4 cuts, Ph.D Thesis, Univ. Barcelona, 2011.

[29] C. Fité, J. Tejero, J.F. Izquierdo, F. Cunill, Kinetics of the liquid-phase synthesis of ethyl tert-butyl ether (ETBE), Ind. Eng. Chem. Res. 33 (1994) 581–591.

[30] N. Oktar, M. Mürtezaoğlu, G. Doğu, I. Gönderten, T. Doğu, Etherification rates of 2-methyl-2-butene and 2-methyl-1-butene with ethanol for environmentally clean gasoline production, J. Chem. Biotechnol. 74 (1999) 155–161.

[31] R. Soto, C. Fité, E. Ramírez, R. Bringué, F. Cunill, Equilibrium of the simultaneous etherification of isobutene and isoamylenes with ethanol in liquid-phase, Chem. Eng. Res. Des. 92 (2014) 644–656.

[32] C. Gómez, F. Cunill, M. Iborra, J.F. Izquierdo, J. Tejero, Experimental study of the simultaneous synthesis of methyl tert-butyl ether and ethyl tert-butyl ether in liquid phase, Ind. Eng. Chem. Res. 36 (1997) 4756–4762.

[33] F. Ancillotti, M.M. Mauri, E. Pescarollo, L. Romagnoni, Mechanism in the reaction between olefins and alcohols, J. Mol. Catal. 4 (1978) 37-48.

[34] F. Ancillotti, M.M. Mauri, E. Pescarollo, Ion exchange resins catalyzed addition of alcohols to olefins, J. Catal. 46 (1977) 49-57.

[35] A. Fitó, J.A. Linnekoski, Equilibrium of simultaneous tert-amyl ethyl ether and tert-amyl alcohol formation reactions, Ph.D Thesis, Helsinki Univ. Technol., 2008.

[36] R.L. Mason, R.F. Gunst, J.L. Hess, Statistical design and analysis of experiments: with applications to engineering and science, second ed., John Wiley & Sons, New Jersey, 2003.

[37] R.H. Myers, D.C. Montgomery, C.M. Anderson-Cook, Response surface methodology: process and product optimization using designed experiments. third ed., John Wiley & Sons, New Jersey, 2009.

[38] N. R. Draper, H. Smith, Applied regression analysis, second ed., John Wiley & Sons, New York, 1998.

[39] A.I. Khuri and J.A. Cornell, Response surfaces: designs and analyses, first ed., M. Dekker, New York, 1987.

[40] E.C. Harrington, The desirability function, Ind. Qual. Control. 21 (1965) 494–498.

[41] G. Derringer, R. Suich, Simultaneous optimization of several response variables, J. Qual. Technol. 12 (1980) 214-219.

[42] L.K. Rihko, A.O.I. Krause, Reactivity of isoamylenes with ethanol, Appl. Catal. A: Gen. 101 (1993) 283–295.

[43] M. Iborra, J. Tejero, M.B. El-Fassi, F. Cunill, J.F. Izquierdo, C. Fité. Experimental study of the liquid-phase syntheses of methyl tert.butyl ether (MTBE) and tert-butyl alcohol (TBA). Ind. Eng. Chem. Res. 41 (2002) 5359–5365.

[44] J. Tejero, A. Calderón, F. Cunill, J.F. Izquierdo, M. Iborra, The formation of byproducts in the reaction of synthesis of isopropyl tert-butyl ether from isopropyl alcohol and

isobutene on an acidic macroporous copolymer, React. Funct. Polym. 33 (1997) 201–209.

[45] A. Delion, Hydration of isopentenes in an acetone environment over ion-exchange resin: Thermodynamic and kinetic analysis, J. Catal. 103 (1987) 177–87.

[46] V.J. Cruz , R. Bringue, F. Cunill, J.F. Izquierdo, J. Tejero, M. Iborra, C. Fité, Conversion, selectivity and kinetics of the liquid-phase dimerisation of isoamylenes in the presence of C1 to C5 alcohols catalysed by a macroporous ion-exchange resin, J. Catal. 238 (2006) 330–341.

[47] R.S. Karinen, M.S. Lylykangas, A.O.I. Krause., Reaction equilibrium in the isomerization of 2,4,4-trimethyl pentenes, Ind. Eng. Chem. Res. 40 (2001) 1011–1015.

[48] T.W.G Solomons, C.B. Fryhle, Organic chemistry, tenth ed., John Wiley and Sons, New York, 2000.

[49] V.J. Cruz, J.F. Izquierdo, F. Cunill, J. Tejero, M. Iborra, C. Fité, Acid ion-exchange resins catalysts for the liquid-phase dimerization/etherification of isoamylenes in methanol or ethanol presence, React. Funct. Polym. 65 (2005) 149–160.

[50] H. Hamid, M.A. Ali, Handbook of MTBE and other gasoline oxygenates, first ed., M. Dekker, New York, 2004.

Table 1. Relevant properties of potential gasoline additives [19, 21-26].

Compound	(RON+MON)/ 2	Solubility in water (g/L water)	Oxygen Content (wt.%)	bRVP (psi)	T_b (K)	Reactivity[a]
MTBE	110	48.5	18.2	8	328	2.6
ETBE	112	26.0	15.7	4	345	8.1
TAME	105	20.0	15.7	2	361	7.9
TAEE	100	4.0	13.8	2	375	-
Methanol	116	∞	50	60	338	1
Ethanol	115	∞	34.8	18	351.3	3.4
IB	Low	0.388	0	66	266	55
2M2B	91	0.190	0	15	304.1	85
2M1B	92	0.130	0	19	311.6	70
TBA	101	∞	21.6	10	356	1.1
TAA	97[b]	120.0	18.2	0.32[c]	375	-
TMP-1 and TMP-2	~100	0	0	1.56[c]	374.5	-
Hydrogenated C_5 dimer	95	-	0	0.5	420	-

[a] *Hydroxyl reaction rate coefficient: $k \cdot 10^{12}$ $cm^3 \cdot molecule^{-1} \cdot s^{-1}$*

[b] *RON value, because (RON+MON)/2 was not available*

[c] *Vapor pressure value at 293 K, because blending Reid vapor pressure was not available*

Table 2. Fitted parameters of the significant coded variables for the response surface as the empirical model of TAEE and ETBE yield from IA and IB, respectively

Terms	Y_{IA}^{TAEE}			Y_{IB}^{ETBE}		
	Coefficient	Standard error	*p*-value	Coefficients	Standard error	*p*-value
β_0	41.598	0.486	$3.48 \cdot 10^{-43}$	87.612	0.573	$1.94 \cdot 10^{-53}$
β_1 (T)	–7.228	0.384	$3.10 \cdot 10^{-20}$	–3.982	0.518	$3.56 \cdot 10^{-09}$
β_2 (x_A)	16.011	0.387	$5.99 \cdot 10^{-32}$	9.160	0.523	$1.69 \cdot 10^{-19}$
β_3 (x_{C4})	–2.484	0.387	$1.93 \cdot 10^{-07}$	–3.646	0.523	$3.10 \cdot 10^{-08}$
β_{22} (x_A^2)	–6.260	0.596	$1.62 \cdot 10^{-12}$	–6.807	0.776	$1.42 \cdot 10^{-10}$
β_{33} (x_{C4}^2)	1.470	0.596	$1.85 \cdot 10^{-02}$	-	-	-
β_{12} ($T \cdot x_A$)	–2.880	0.519	$2.82 \cdot 10^{-06}$	1.470	0.702	$4.31 \cdot 10^{-02}$
β_{23} ($x_A \cdot x_{C4}$)	2.642	0.474	$2.59 \cdot 10^{-06}$	4.100	0.641	$1.80 \cdot 10^{-07}$
Adjusted R^2		98.14			92.51	
Model F-value		325.66			89.47	
Critical F-value		$1.4 \cdot 10^{-30}$			$1.7 \cdot 10^{-20}$	

Table 3. Fitted parameters of the significant coded variables for the response surface as the empirical model of TAEE and ETBE yield from EtOH

Terms	Y_{EtOH}^{TAEE}			Y_{EtOH}^{ETBE}		
	Coefficient	Standard Error	*p*-value	Coefficients	Standard Error	*p*-value
β_0	23.436	0.339	$6.99 \cdot 10^{-40}$	45.4741	0.382	$1.38 \cdot 10^{-51}$
β_1 (T)	–3.509	0.267	$2.72 \cdot 10^{-15}$	–1.053	0.512	0.047
β_2 (x_A)	–4.173	0.270	$1.76 \cdot 10^{-17}$	–22.517	0.517	$1.08 \cdot 10^{-34}$
β_3 (x_{C4})	–8.823	0.270	$2.25 \cdot 10^{-28}$	12.460	0.517	$4.86 \cdot 10^{-25}$
β_{22} (x_A^2)	–5.292	0.415	$6.50 \cdot 10^{-15}$	-	-	-
β_{33} (x_{C4}^2)	0.942	0.415	$2.93 \cdot 10^{-02}$	-	-	-
β_{13} (T·x_{C4})	1.391	0.362	$4.75 \cdot 10^{-04}$	-	-	-
β_{23} (x_A·x_{C4})	4.396	0.330	$1.81 \cdot 10^{-15}$	–4.469	0.633	1.7710^{-8}
Adjusted R^2		97.71			98.33	
Model F-value		262.53			633.45	
Critical F-value		$6.33 \cdot 10^{-29}$			$6.73 \cdot 10^{-35}$	

Table 4. Values of individual desirability functions $d_n(Y_n(z))$, overall desirability $D(x)$ and predicted etherification yields for the optimal experimental conditions (first row) and other interesting experimental conditions (following rows).

T [K]	x_A	x_{C4}	$d\left(Y_{EtOH}^{TAEE}\right)$	$d\left(Y_{IA}^{TAEE}\right)$	$d\left(Y_{IB}^{ETBE}\right)$	$d\left(Y_{EtOH}^{ETBE}\right)$	$D(x)$	Y_{EtOH}^{TAEE}	Y_{IA}^{TAEE}	Y_{IB}^{ETBE}	Y_{EtOH}^{ETBE}
323	0.462	0.333	0.92	0.79	1	0.45	0.76	39.8	49.0	94.2	38.2
323	0.5	0.333	0.88	0.86	1	0.39	0.74	38.1	53.1	95.4	34.1
323	0.5	0.5	0.62	0.8	0.98	0.54	0.72	26.9	49.1	91.7	46.5
323	0.5	0.666	0.41	0.78	0.94	0.69	0.67	17.7	48.1	88.1	58.9
323	0.55	0.333	0.81	0.93	1	0.34	0.71	35.1	57.4	95.9	28.6
323	0.666	0.5	0.40	1	0.99	0.28	0.58	17.5	61.8	92.7	24.1

FIGURE CAPTIONS

Figure 1. Full reaction network. Grey colored area stands out the main reactions that take place.

Figure 2. Effect of the temperature on the reactants conversion at equilibrium under different initial compositions: (a) $R_{A/O}=R_{C4/C5}=1$; (b) $R_{A/O}=0.5$, $R_{C4/C5}=1$; (c) $R_{A/O}=2$, $R_{C4/C5}=0.5$; (d) $R_{A/O}=R_{C4/C5}=2$. Errors bars refer to the 95% confidence interval.

Figure 3. Effect of the temperature on the reactants selectivity toward products at equilibrium under different initial compositions: (a) $R_{A/O}=R_{C4/C5}=1$; (b) $R_{A/O}=1$, $R_{C4/C5}=0.5$; (c) $R_{A/O}=1$, $R_{C4/C5}=2$; (d) $R_{A/O}=R_{C4/C5}=2$

Figure 4. Effect of the initial $R_{A/O}$ on the reactants conversion at equilibrium at different temperatures and fixed initial $R_{C4/C5}=1$: (a) IB; (b) EtOH; (c) IA

Figure 5. Effect of the initial $R_{A/O}$ on the reactants selectivity at equilibrium at fixed initial $R_{C4/C5}=1$: (a) 353 K; (b) 343 K

Figure 6. Effect of the initial $R_{C4/C5}$ on the reactants conversion at equilibrium obtained under different experimental conditions: (a) $R_{A/O}=0.5$ and 333 K; (b) $R_{A/O}=2$ and 343 K; (c) $R_{A/O}=1$ and 343 K; (d) $R_{A/O}=2$ and 323 K

Figure 7. Effect of the initial $R_{C4/C5}$ on the reactants selectivities at equilibrium obtained under different experimental conditions: (a) 353 K and $R_{A/O}=2$; (b) 353 K and $R_{A/O}=0.5$

Figure 8. Tertiary alcohols formation: (a) Effect of temperature at $R_{A/O}= R_{C4/C5}=1$; (b) Effect of $R_{A/O}$ at 353 K and $R_{C4/C5}=1$; (c) Effect of $R_{C4/C5}$ at 343 K and $R_{A/O}=2$

Figure 9. Dimers and codimers formation: (a) Mole evolution at $R_{A/O}=0.5$, $R_{C4/C5}=1$ and 353 K using 4g of Amberlyst 35; (b) Effect of $R_{C4/C5}$ on olefins selectivity toward products at 353 K and $R_{A/O}=0.5$

Figure 10. Comparison of experimental with predicted yield values at equilibrium for all experimental conditions: (a) Y_{IA}^{TAEE}; (b) Y_{IB}^{ETBE}; (c) Y_{EtOH}^{TAEE}; (d) Y_{EtOH}^{ETBE}

Figure 11. Plot of some obtained response surfaces and experimental points: (a) Y_{IB}^{ETBE} vs. x_A and T at $x_{C4}=0.5$; (b) Y_{IA}^{TAEE} vs. x_A and T at $x_{C4}=0.5$. Symbols (○) refer to the experimental yield data.

Figure 12. Overlaid Contour Plot (OCP) for etherification yields at (a) $x_{C4}=0.333$ and (b) $x_{C4}=0.666$. Grey shadowed area gathers the optimal conditions for the simultaneous production of ETBE and TAEE. (▬) Y_{EtOH}^{TAEE};(▪▪▪) Y_{IA}^{TAEE};(---) Y_{IB}^{ETBE};(–·–) Y_{EtOH}^{ETBE}

Figure 13. Contour plot for the obtained overall desirability $D(x)$ at $x_{C4}=0.333$.

Figure 1.

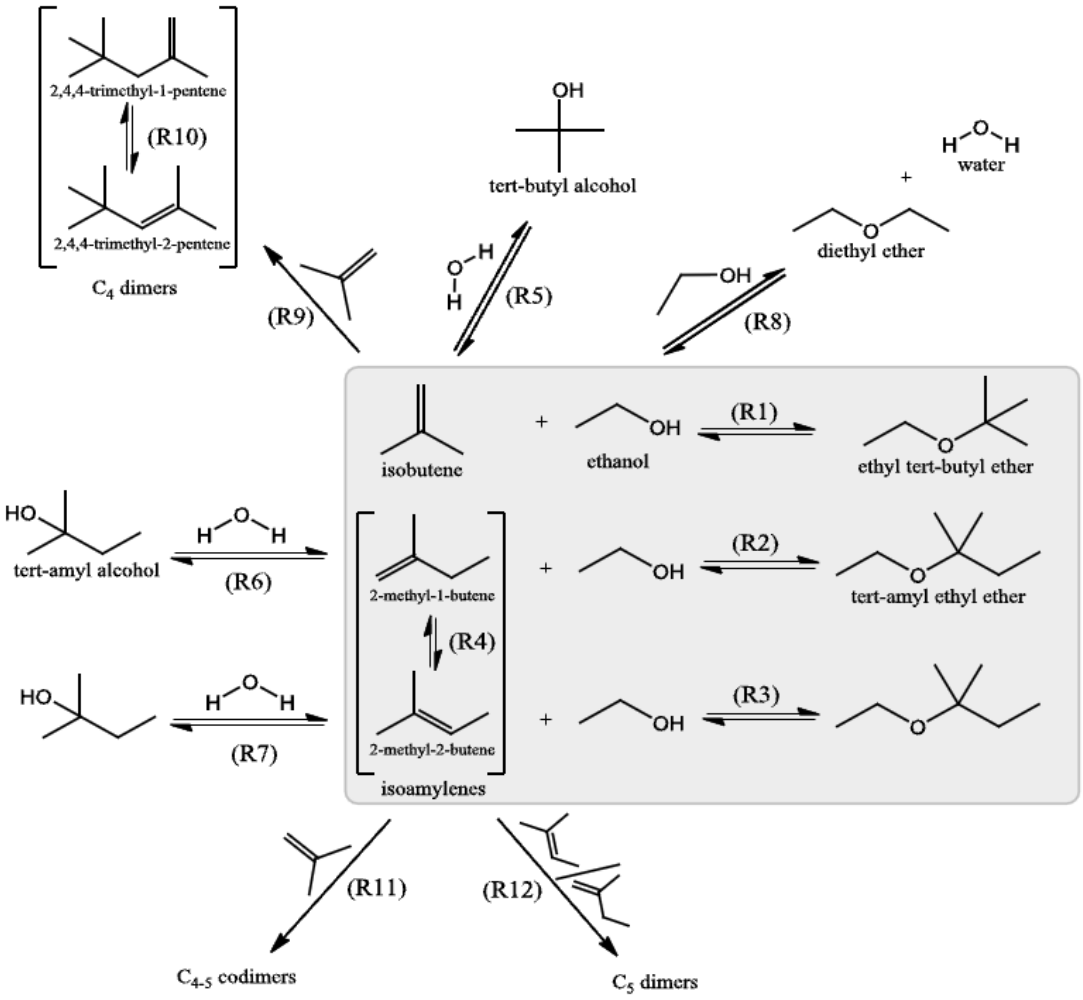

Figure 2.

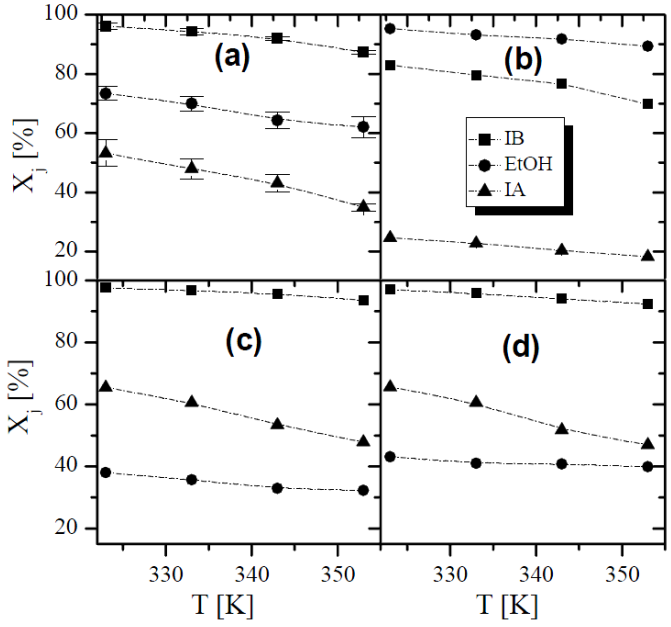

Figure 3.

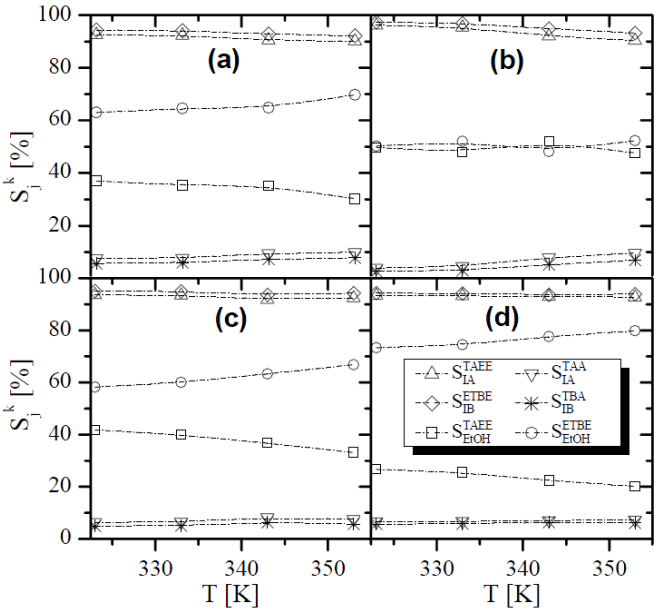

Figure 4.

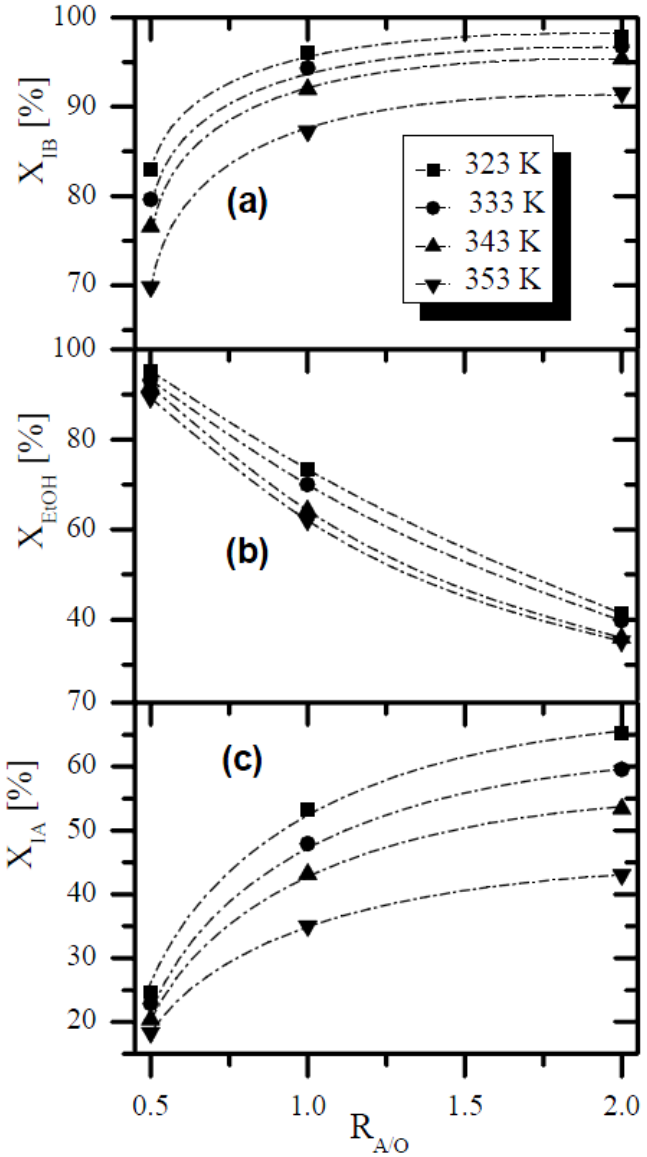

Figure 5.

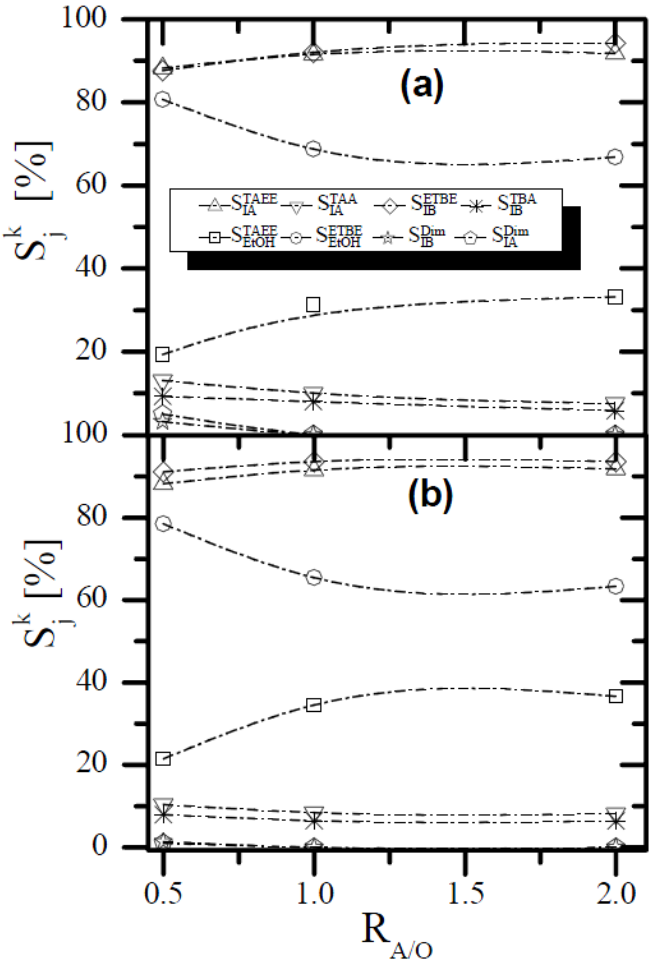

Figure 6.

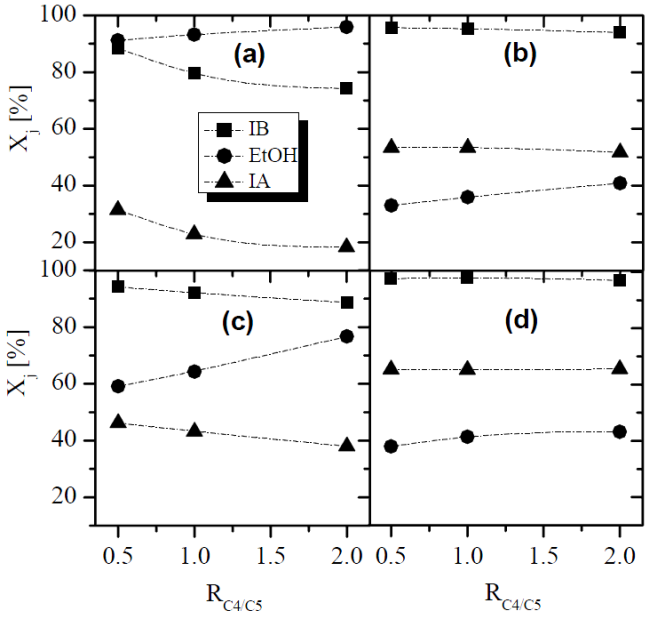

Figure 7.

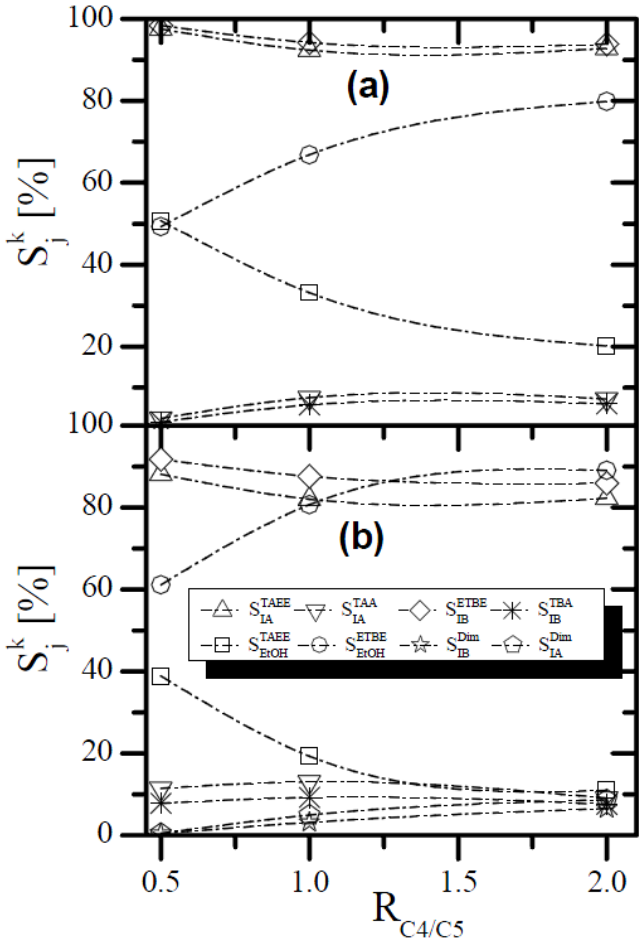

Figure 8.

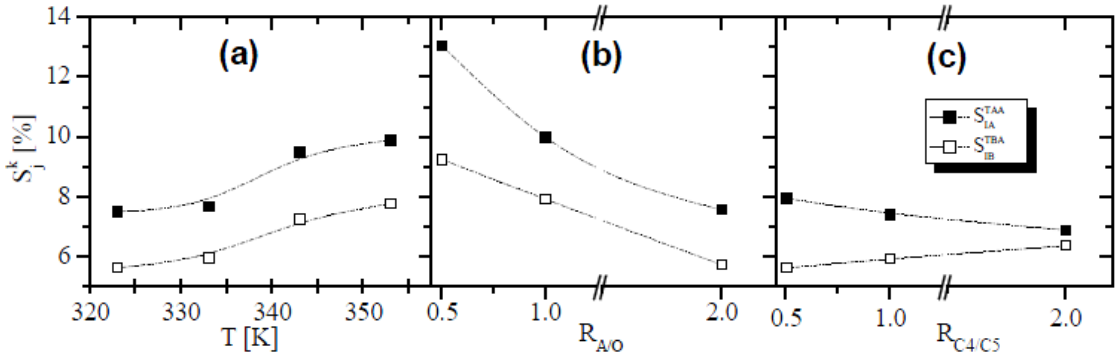

Figure 9.

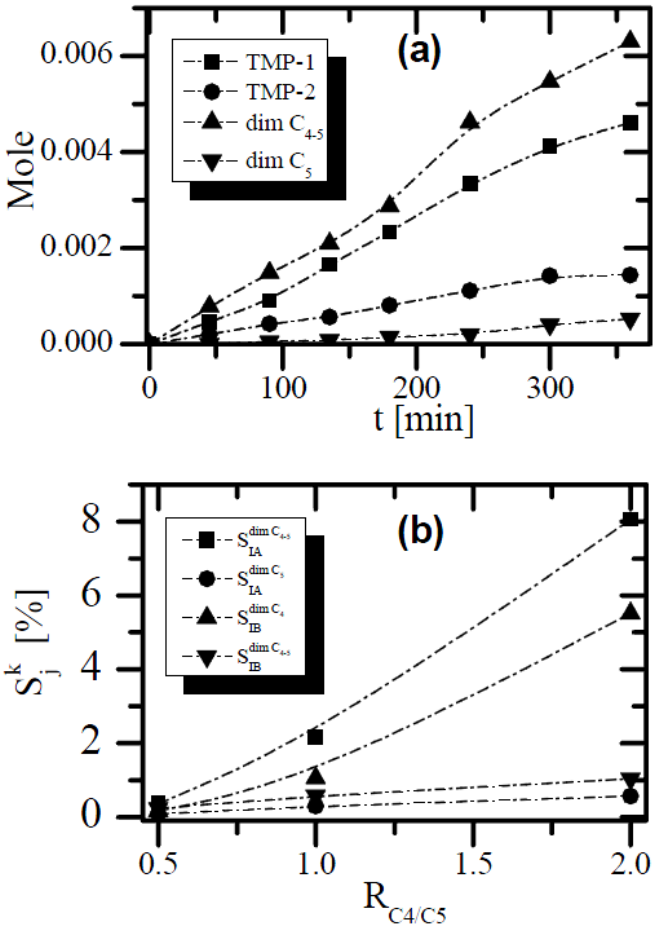

Figure 10.

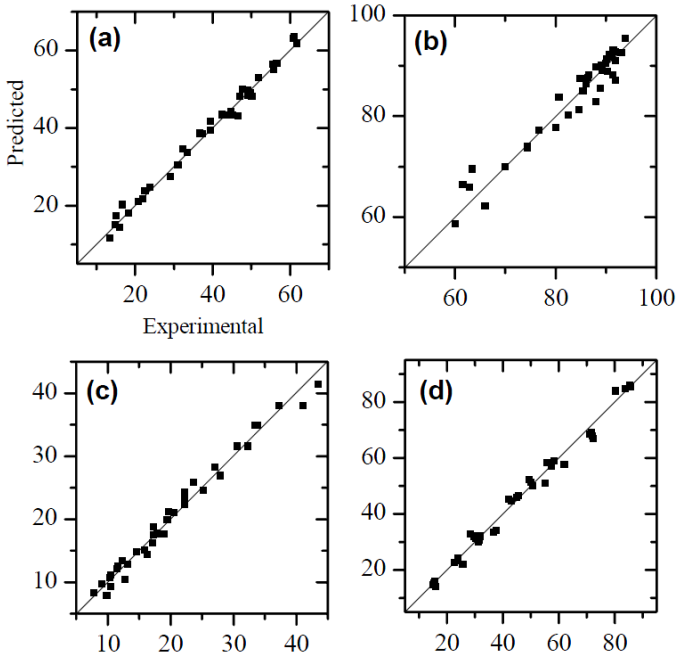

Figure 11.

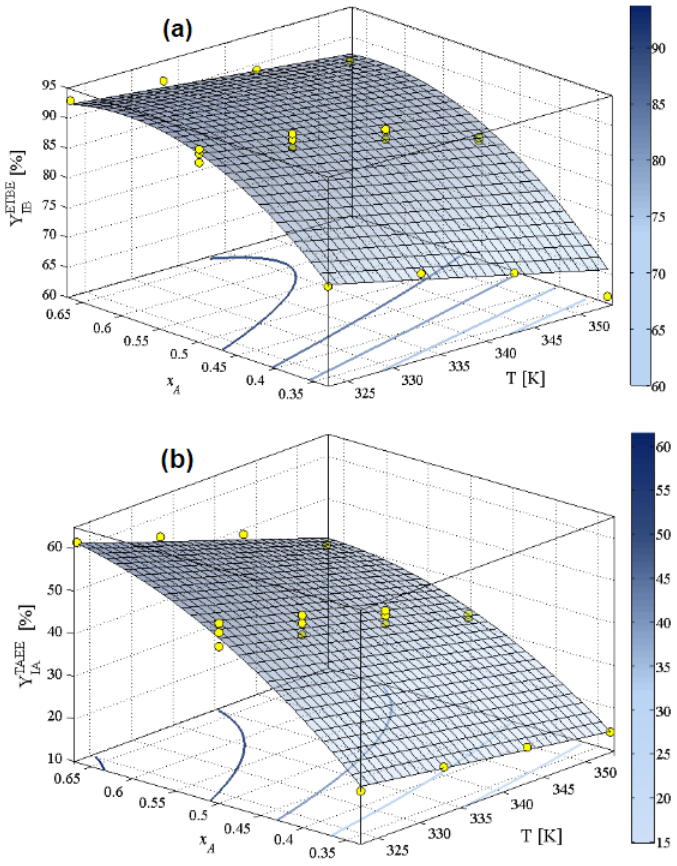
(a)
Y_{IE}^{ETBE} [%]
95
90
85
80
75
70
65
60
0.65
0.6
0.55
0.5
0.45
0.4
0.35
x_A
325
330
335
340
345
350
T [K]
90
85
80
75
70
65
60
(b)
Y_{IA}^{TAEE} [%]
60
50
40
30
20
10
0.65
0.6
0.55
0.5
0.45
0.4
0.35
x_A
325
330
335
340
345
350
T [K]
60
55
50
45
40
35
30
25
20
15

Figure 12.

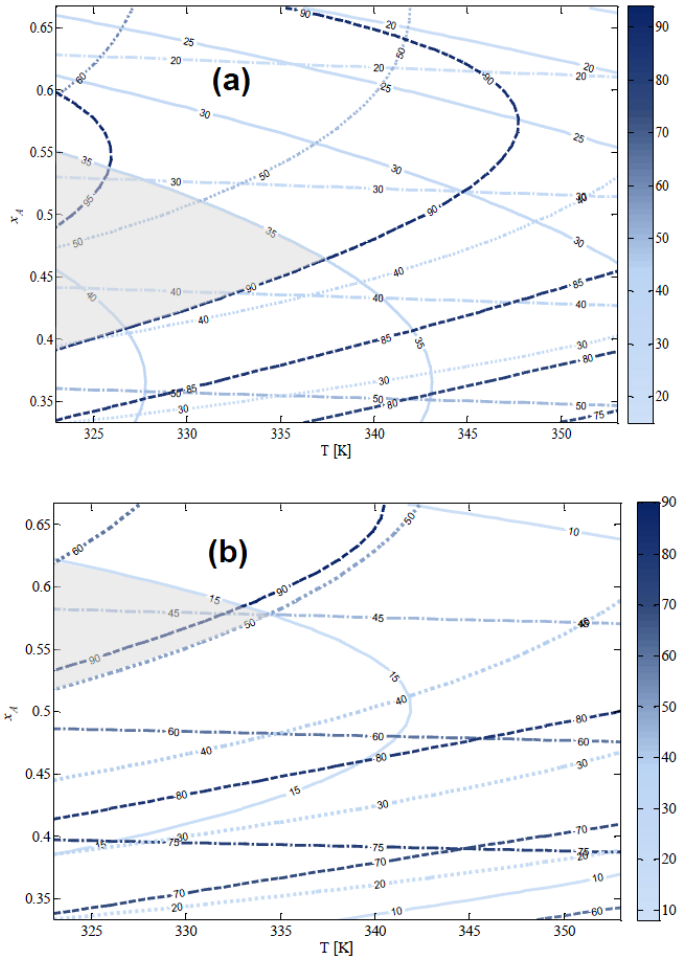

Figure 13.

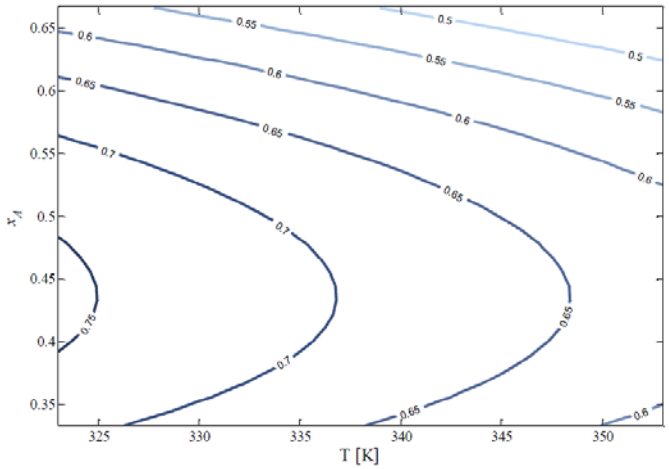

Supplementary Material

Appendix 1. Experimental yield data empirically modeled. Errors refer to a 95% probability level for the replicated experiments.

$R_{C4/C5}$	$R_{A/O}$	T (K)	Y_{IA}^{TAEE}	Y_{IB}^{ETBE}	Y_{EtOH}^{TAEE}	Y_{EtOH}^{ETBE}
0.5	0.5	323	31.06	85.47	43.47	49.40
0.5	0.5	333	29.15	84.62	41.14	49.97
0.5	0.5	343	23.91	80.00	33.48	50.22
0.5	0.5	353	21.91	74.46	32.27	50.78
0.5	1	323	51.94	93.78	37.24	37.69
0.5	1	333	47.17	91.90	33.91	36.83
0.5	1	343	42.42	89.09	30.59	28.38
0.5	1	353	36.75	84.91	26.99	29.67
0.5	2	323	60.87	90.65	22.21	15.71
0.5	2	333	55.60	89.96	20.51	15.30
0.5	2	343	49.17	90.25	17.89	15.00
0.5	2	353	46.60	91.92	16.38	15.93
1	0.5	323	22.50	76.72	23.65	72.77
1	0.5	333	20.94	74.40	22.17	72.47
1	0.5	343	18.37	70.03	19.71	72.04
1	0.5	353	16.81	61.61	18.33	71.11
1	1	323	49.74±3.84	91.30±1.55	27.85±0.62	45.69±2.26
1	1	333	44.82±3.21	89.28±1.63	25.26±0.36	44.99±1.73
1	1	343	39.46±2.22	86.02±1.22	22.20±0.44	42.10±2.60
1	1	353	32.34±0.73	80.66±0.39	19.49±0.91	42.00±2.4
1	2	323	61.70	93.06	17.26	24.05
1	2	333	55.83	91.87	15.91	23.88
1	2	343	49.21	89.24	13.12	22.66
1	2	353	39.44	86.35	12.78	25.75
2	0.5	323	16.70	63.50	11.44	85.45
2	0.5	333	15.96	62.80	10.35	85.60
2	0.5	343	14.95	62.01	10.48	83.87
2	0.5	353	13.43	60.13	9.86	80.28
2	1	323	50.18	91.35	19.02	58.27
2	1	333	45.21	88.92	17.14	55.81
2	1	343	37.44	87.94	14.61	62.08
2	1	353	33.53	82.57	12.32	57.29
2	2	323	61.08	91.49	11.62	31.94
2	2	333	56.58	90.20	10.47	30.47
2	2	343	47.70	87.97	9.15	31.67
2	2	353	44.16	86.64	7.87	31.19

Appendix 2. Residuals plots obtained for the modeled yield data at all assayed temperature and initial composition.